Talanta 85 (2011) 2695–2699

Contents lists available at ScienceDirect

Talanta

journal homepage: www.elsevier.com/locate/talanta

Short communication

Facile synthesis of fluorescent Au@SiO_2 nanocomposites for application in cellular imaging

Zhengyong Zhang, Peng Zhang, Kai Guo, Guohai Liang, Hui Chen, Baohong Liu, Jilie Kong*

Department of Chemistry and Institutes of Biomedical Sciences, Fudan University, Shanghai, 200433, China

ARTICLE INFO

Article history:
Received 18 March 2011
Received in revised form 10 June 2011
Accepted 11 June 2011
Available online 17 June 2011

Keywords:
Au@SiO_2
Fluorescent nanocomposite
Fluorescence imaging

ABSTRACT

A novel fluorescent Au@SiO_2 nanocomposite, with average size of ca. 30 nm in the diameter, was prepared via a simple microemulsion method. Additionally, transmission electron microscopy (TEM), UV–Vis absorption spectra, Fourier transform infrared (FT-IR) spectra and fluorescence spectra were used to characterize this nanocomposite. This newly synthesized, silica-wrapped, gold nanocluster has the following advantages: good water solubility, exceptional biocompatibility, favorable surface properties and excellent fluorescence properties. Because of these advantages, a Au@SiO_2 nanocomposite is exceptionally suitable for biological applications. In this study, cellular imaging, as a form of biological application, has been fully investigated, and it was discovered, after covalent conjugation of folic acid (FA), that the nanocomposite effectively recognized over expressed folic acid receptors (FARs) on the HeLa cell's surface. Therefore, this fluorescent Au@SiO_2 nanocomposite could be used as a new fluorescent probe for selective biological imaging.

1. Introduction

In recent years, monolayer protected gold nanoparticles (Au-NPs) have gained significant attention owing to their unique electronic and optical properties compared with conventional organic dyes and fluorescence proteins [1–4]. Specifically, photoluminescence quantum yields (QYs) have been enhanced by up to eight orders of magnitude in comparison to that of bulk gold by use of gold monolayer-protected clusters [5,6]. With their exceptional fluorescence properties, these fluorescent gold nanoclusters (Au-NCs) are also called gold quantum dots [7] and are used for mercury(II)ion and protein detections [8,9]. Fluorescent Au-NCs represent a great value because of their high photoluminescence quantum yields; however, they are generally susceptible to their external environment, are unstable in diverse media, and can be difficult to functionalize further [10]. Additionally, due to the small sizes of the alkanethiol ligand protected Au-NCs (diameters are no larger than 3 nm), the purification progress is complex and difficult [11]. In other words, these defects limit the application of Au-NCs in the biology field.

Encapsulation of the alkanethiol ligand protected Au-NCs with silicon dioxide can overcome the above-mentioned defects. A wide variety of silica coating and modification procedures have been developed for various nanoparticles during the past decade, with significant progress particularly in the encapsulation of quantum dots (QDs) and metal nanocrystals with a protective shell [12–14]. QDs have some advantages, for instance, continuous adsorption spectra and sharp emission spectra [15–17], however, QDs are generally susceptible to external environment and have or potential biological toxicity may be due to their intrinsic physicochemical properties, or result from the release of toxic components during breakdown [18,19]. Plus Au, Ag nanoparticles are most commonly used as a strong enhancement effect for surface-enhanced Raman scattering (SERS) [20,21]. Until now, little study is done on the encapsulation of fluorescent Au-NCs with silicon dioxide shell.

Herein, we describe a straightforward method for the preparation of fluorescent Au-NCs with silica coating outer shells. After silica coating, the nanocomposite is easy to functionalize; furthermore, its chemical and fluorescence stabilities become enhanced under the protection of the outer surface. The fluorescent Au@SiO_2 nanocomposite is stable in aqueous solution at 4 °C for at least three months. Additionally, we demonstrate the application of bioconjugated Au-NCs@SiO_2 nanocomposites as bioprobes for cellular imaging.

2. Experimental

2.1. Reagents and materials

Chloroauric acid ($HAuCl_4 \cdot 3H_2O$), sodium hydroxide (NaOH), trisodium tetraborate, cyclohexane, n-hexanol, tetraethyl orthosilicate (TEOS), and 25% ammonia were purchased from Sinopharm

* Corresponding author. Tel.: +86 21 65642138; fax: +86 21 65641740.
E-mail address: jlkong@fudan.edu.cn (J. Kong).

0039-9140/$ – see front matter © 2011 Elsevier B.V. All rights reserved.
doi:10.1016/j.talanta.2011.06.032

Chemical Reagent Co., Ltd. (Shanghai, China). Triton X-100 and 3-(4,5-dimethylthiazol-2yl)-2,5-diphenyltetrazolium bromide (MTT) were purchased from Shanghai Sangon Biotechnology Co. (Shanghai, China). Tetrakis (hydroxymethyl) phosphonium chloride (THPC) was purchased from TCI Development Co., Ltd. (Shanghai, China). 11-Mercaptoundecanoic acid (11-MUA), 3-aminopropyl triethoxysilane (APTES), folic acid (FA), N-ethyl-N′-(3-(dimethylamino)propyl)carbodiimide (EDC) and sulfo-N-hydroxysuccinimide (sulfo-NHS) were obtained from Sigma Aldrich Company (USA). Double distilled water was used throughout.

2.2. Synthesis of small Au nanoparticles (Au-NPs)

The small Au-NPs were synthesized through the reduction of $HAuCl_4 \cdot 3H_2O$ with THPC. To an aqueous solution (45 mL) was added 1 mol/L NaOH (0.5 mL), followed by the addition of a THPC solution (1 mL) that was prepared by adding an 80% THPC solution (12 μL) to water (1 mL). The mixture was stirred 5 min, followed by the rapid addition of an aqueous solution of $HAuCl_4 \cdot 3H_2O$ (1.5 mL, 1 wt%). Next, the solution was vigorously stirred for 15 min and stored at 4 °C for further use.

2.3. Preparation of Au nanoclusters protected with 11-mercaptoundecanoic acid (11-MUA)

The Au-NCs were obtained by introducing 11-MUA to the solution of Au-NPs. In brief, to 25-mL volumetric flasks were added the as-prepared Au-NPs (5.0 mL), trisodium tetraborate (1 mL, 50 mM, pH 9.2), and the 11-MUA stock solution (1 mL, 100 mM), and then the mixtures were diluted to 10.0 mL with water. The solution was left to react for 72 h in the dark at room temperature. The resulting 11-MUA protected Au-NCs exhibited strong fluorescence under UV lamp, and the 11-MUA protected Au-NCs were subsequently centrifuged (14,000 rpm) for 20 min through a filter with a cutoff of 10 KDa (membrane nominal pore size ~1 nm) to remove any excess thiol acid. Finally, the oily precipitates on the filter were resuspended in an aqueous solution.

2.4. Preparation of 11-MUA Au-NCs@SiO_2 nanocomposites

A water-in-oil microemulsion was prepared by mixing cyclohexane (7.5 mL), Triton X-100 (1.77 mL), and n-hexanol (1.80 mL) and stirring for 30 min. Next, 1 mL of the 11-MUA Au-NCs aqueous solution was slowly added with continued agitation over about 30 min. Subsequently, 25% ammonia water (60 μL) was added to the solution, and 5 min later, TEOS (100 μL) was injected into the reaction solution. The reaction was stirred for an additional 24 h in the dark. Acetone (10 mL) was added to break up the microemulsion and precipitate the 11-MUA Au-NCs@SiO_2 nanoparticles.

In order to obtain the amine functionalized nanocomposites, (3-aminopropyl)triethoxysilane (APTES) was used to functionalize the product surface; 10–15 μL of APTES was added to the 11-MUA Au-NCs@SiO_2 reaction solution after reacting for 24 h. By continuing to stir for 19–20 h in the dark, the amine functional 11-MUA Au-NCs@SiO_2 conjugates were obtained after adding acetone (10 mL) to break up the microemulsion. Next, the resulting products were centrifuged at 10,000 rpm, washed several times with ethanol and deionized water, and freeze dried for future use.

2.5. Bioconjugation of 11-MUA Au-NCs@SiO_2 nanoparticles with folic acid (FA)

Briefly, 1 mL of FA (1 mM) aqueous solution was activated for 30 min with EDC and sulfo-NHS, where the final molar concentrations were 200 mM and 50 mM, respectively. The amine functionalized 11-MUA Au-NCs@SiO_2 nanocomposites (8 mg) were dispersed in the activated FA solution by vortex mix technology (30 s), and then the reaction was stirred for 2–3 h at room temperature under gentle rotation in the dark. The FA-conjugated nanoparticles were purified by centrifugation at 10,000 rpm for 10–15 min, washed more than 3 times with deionized water, then resuspended in 10 mM (phosphate buffered saline) PBS buffer.

2.6. Cell cultivation

Human cervical carcinoma (HeLa) cells were routinely cultured at 37 °C in flasks containing Dulbecco's Modified Eagle Medium (DMEM) with 5% fetal bovine serum (FBS) in a humidified atmosphere and with 5% CO_2 in a Themo culturist. Cells were plated in a tissue culture flask with 100% humidity.

2.7. Cytotoxicity assay

In vitro, cytotoxicity was evaluated by performing 3-(4,5-dimethylthiazol-2yl)-2,5-diphenyltetrazolium bromide (MTT) assays in the HeLa cells. Cells were seeded at 10^4 per cell into a 96-well cell culture plate in DEME with 5% fetal bovine serum at 37 °C and with 5% CO_2 for 24 h. Next, the cells were incubated with different concentrations (80 μg/mL, 200 μg/mL, 400 μg/mL, and 800 μg/mL) of the 11-MUA Au-NCs@SiO_2-FA nanoparticles for 24 h. After that time, MTT (100 μL, 5 mg/mL) was added to each well, and the plate was incubated for another 4 h at 37 °C. The assays were performed according to the manufacturer's instructions. The absorbance of MTT at 492 nm was measured by an automatic ELISA analyzer (SPR-960).

2.8. Laser scanning confocal fluorescence microscopy

After the HeLa cells were cultured in DMEM with 5% FBS at 37 °C and with 5% CO_2 for 24 h, the 11-MUA Au-NCs@SiO_2 (FA) (5 μL) were introduced into the culture dish containing the HeLa cells for 30 min at 37 °C and with 5% CO_2. Fluorescence imaging was performed with a Leica TCs SP5 microscope and using a Leica application suite, advanced fluorescence confocal scanning system. A 40× dry objective lens was used. Excitation of the 11-MUA Au-NCs@SiO_2 (FA) was performed with a laser at $\lambda = 405$ nm, and emissions were collected using a wavelength range of 485–545 nm.

3. Results and discussion

The 11-MUA Au-NCs were characterized by a transmission electron microscope (TEM) (Fig. 1a). TEM images show that the obtained Au-NCs were narrowly distributed and well dispersed, with an average diameter size of ca. 2 (±0.2) nm. In a typical water-in-oil reverse microemulsion synthesis, cyclohexane serves as the "oil" phase in which the surfactant, preferably Triton X-100, and co-surfactant, n-hexanol, were dissolved [22]. Hydrophilic, ligated 11-MUA Au-NCs were mixed within the water and then added into the reaction solution slowly. Here, the 11-MUA Au-NCs acted as silica nucleation sites because the nanocomposites could disperse and stabilize in an aqueous solution. This result occurred mainly because the capping agents can form strong covalent, distinctly directional Au–S bonds on the Au-NPs surfaces [23,24]; therefore, they stabilized the clusters in the aqueous solution. Subsequently, the ammonia catalyst was added, TEOS was added into the reaction in the end, and polymerization was then initiated. As revealed in Fig. 1b, the obtained complex nanoparticles were spherical and narrowly distributed and had an average diameter size of ca. 30 nm.

Fig. 2 shows the UV–Vis absorption spectra of bare SiO_2, the 11-MUA Au-NCs and the 11-MUA Au-NCs@SiO_2. No typical absorption was found for the bare silica [25]; in contrast, the 11-MUA Au-NCs

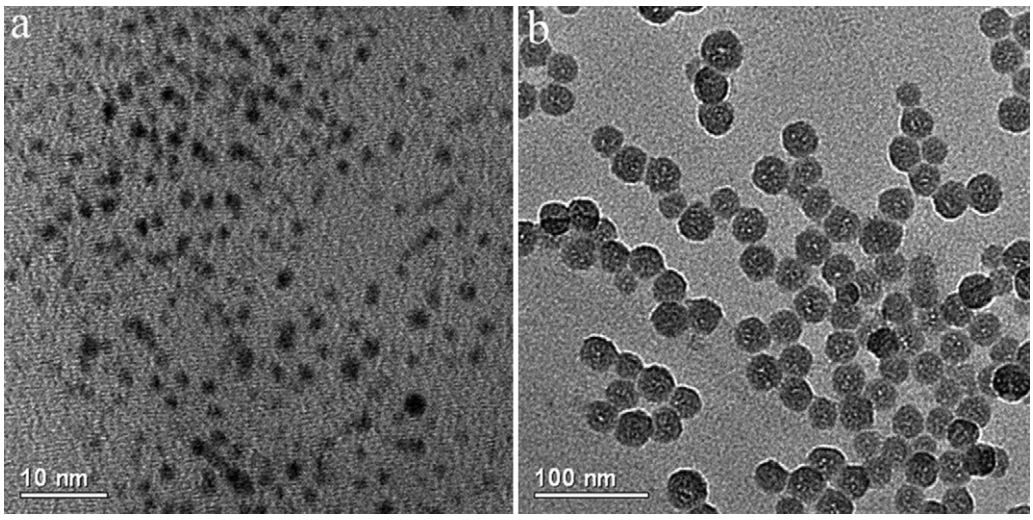

Fig. 1. (a) TEM images of the 11-MUA Au-NCs and (b) 11-MUA Au-NCs@SiO_2.

and 11-MUA Au-NCs@SiO_2 exhibited maximum absorptions at a wavelength of 375 nm. This adsorption peak is suggested to originate from the metal centered (Au $5d^{10}$ to 6sp interband transitions) and/or ligand metal charge transfer transitions, according to the literature [26,27].

Fig. 3 displays the Fourier transform infrared spectroscopy (FT-IR) spectra of the 11-MUA Au-NCs and 11-MUA Au-NCs@SiO_2. Asymmetric (υ_a) and symmetric (υ_s) stretching vibrations of the methylene (CH_2) in the long alkyl chain of 11-MUA were observed at 2924 cm^{-1} and 2849 cm^{-1}, respectively. The prominent feature of the spectra was the carbonyl (C═O) stretching vibration of the carboxylic acid group at 1649 cm^{-1}, whereas the peaks at 1566 cm^{-1} and 1417 cm^{-1} were vibrational modes of the asymmetric (υ_a) and symmetric (υ_s) stretching vibrations of the carboxylate (COO^-), respectively. The peak at 1325 cm^{-1} was characteristic of the scissor vibration (δ) of methylene (CH_2), and the transmission at 1094 cm^{-1} was from the stretching vibration of the 11-MUA carbon–oxygen band (C–O) [28–30]. FT-IR spectra of the obtained fluorescent Au-NCs@SiO_2 nanomaterials demonstrated strong IR bands at 1094 cm^{-1}, which significantly increased due to the asymmetric stretching vibration modes of the Si–O–Si bond [31,32] and confirmed that the siloxane group was introduced into the nanocomposites.

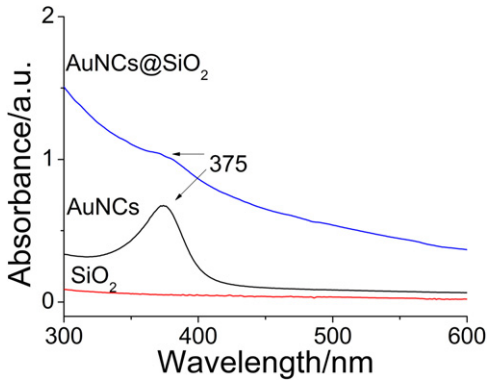

Fig. 2. UV spectra of SiO_2 (red), the 11-MUA Au-NCs (black) and the 11-MUA Au-NCs@SiO_2 (blue). (For interpretation of the references to color in this figure legend, the reader is referred to the web version of the article.)

The 11-MUA Au-NCs and 11-MUA Au-NCs@SiO_2 were also characterized by fluorescence spectra (Fig. 4), and maximum emission peaks around 520 nm and 515 nm were obtained when they were excited at 375 nm. Compared with the 11-MUA Au-NCs, the 11-MUA Au-NCs@SiO_2 showed a 5 nm blue shift, owing to the silica coating confinement effect. When the 11-MUA Au-NCs@SiO_2 were centrifuged at 10,000 rpm for 10 min, they completely precipitated at the bottom of the tube. Comparatively, even after increasing the centrifugation to 14,000 rpm for 40 min, the 11-MUA Au-NCs were still well dispersed. The inset indicated that the fluorescence color of the 11-MUA Au-NCs@SiO_2 solution upon excitation at 365 nm was green, as shown in Fig. 4. (For interpretation of the references

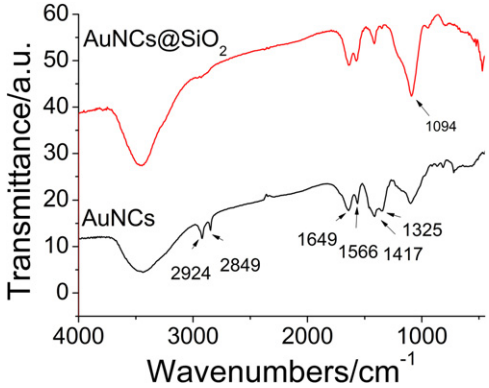

Fig. 3. FTIR spectra of the 11-MUA Au-NCs (black) and 11-MUA Au-NCs@SiO_2 (red). (For interpretation of the references to color in this figure legend, the reader is referred to the web version of the article.)

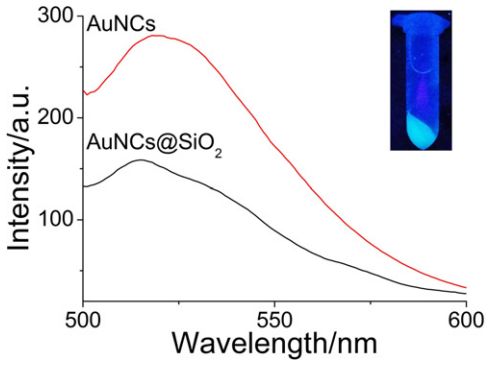

Fig. 4. FL spectra of the 11-MUA Au-NCs (red) and 11-MUA Au-NCs@SiO_2 (black). Photograph of the fluorescence color for the 11-MUA-Au-NCs@SiO_2 under a hand-held UV lamp. Excitation wavelength: 365 nm.

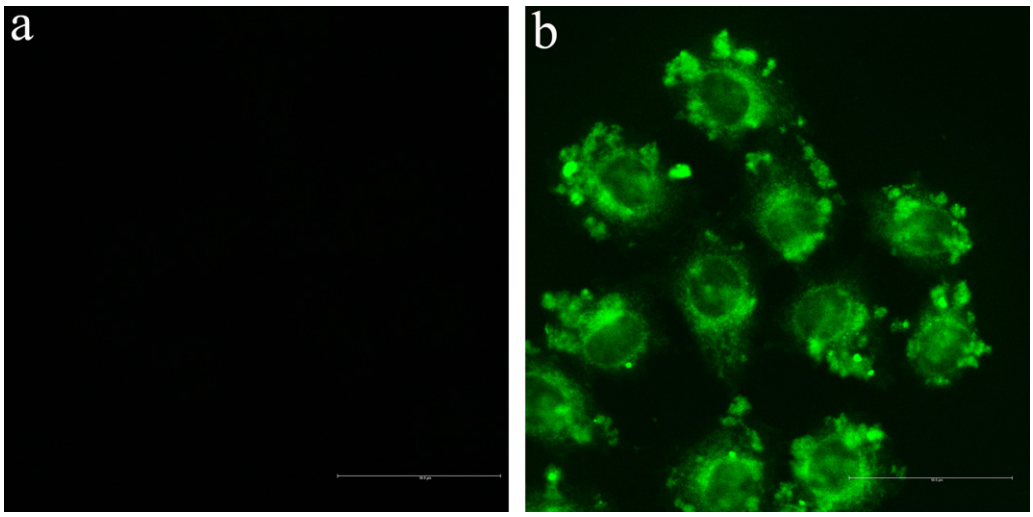

Fig. 5. Confocal microscopy fluorescence images of the HeLa cells treatment with the nanoparticles, (a) 11-MUA Au-NCs@SiO_2 in the HeLa cells and incubated at 37 °C, (b) 11-MUA Au-NCs@SiO_2-FA in the HeLa cells and incubated at 37 °C. The concentration of all of the particles is 80 μg/mL, and the incubation time was 30 min. These images were obtained with using 405-nm laser excitation (scale bar: 50 μm).

to color in the text, the reader is referred to the web version of the article.)

The resulting products of the 11-MUA Au-NCs@SiO_2 were highly attractive for assay applications, particularly in cellular imaging because of their size, biocompatibility and easy modification [33]. In comparison, alkanethiol ligand-protected Au-NCs, such as the 11-MUA Au-NCs, were difficult for targeting cellular imaging because they are small and can be easily endocytosed by cells without high selectivity. The fluorescence Au-NCs@SiO_2, as new biomaterials, has inherited some advantages like high fluorescence properties, favorable surface properties, etc., and they have overcome the difficulties mentioned above.

To investigate the nanocomposite for cellular imaging, the nanomaterial surface was modified with 3-aminopropyl triethoxysilane (APTES, silane reagent) to prepare the amine-functionalized nanocomposite [34]. Next, grafting folic acid (FA) on the functional nanoparticle surface using N-ethyl-N′-(3-(dimethylamino)propyl)carbodiimide (EDC) and sulfo-N-hydroxysuccinimide (sulfo-NHS) as activators occurred [35]. This nanocomposite was used specifically to image human cervical carcinoma cells (HeLa cells) [36,37]. After 30 min of incubation and using the same conditions with and without the nanocomposite at 37 °C, the HeLa cells were observed using a laser scanning confocal microscope (LSCM) (Fig. 5). No fluorescence signal was detected in the control sample labeled without the fluorescent nanocomposite (data not shown). To examine the specific binding of the fluorescent nanocomposite to the overexpressing folic acid receptors (FARs), 11-MUA Au-NCs@SiO_2 were used as a negative control. The confocal fluorescence image showed no distinct fluorescence signal after the 11-MUA Au-NCs@SiO_2 incubated with the HeLa cells at 37 °C (Fig. 5a); however, green fluorescence was observed on the cell membranes when the 11-MUA Au-NCs@SiO_2-FA nanocomposites were added (Fig. 5b), indicating that FA of the nanocomposite recognized the receptor over-expressed in the HeLa cells. Moreover, this observation indicated that the nanocomposites could be used for cellular fluorescence labeling and imaging.

Finally, the cytotoxicity of the complex nanoparticles in the HeLa cells by using a 3-(4,5-dimethylthiazol-2yl)-2,5-diphenyltetrazolium bromide (MTT) cell viability assay has been investigated. Fig. 6 shows the viability of the cells labeled with four different concentrations of the nanocomposites used in the same manner. Even after 24 h of incubation with 800 μg/mL of the fluorescent nanocomposite, the cell viability was more than 87.7%.

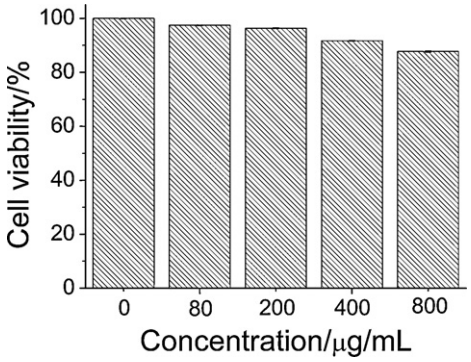

Fig. 6. Cell viability results after incubation of the HeLa cells with various concentrations of the 11-MUA Au-NCs@SiO_2-FA. The percent cell viability is calculated relative to that of the cells without the added nanocomposite, which are defined to have a viability of 100%.

These viabilities are comparable to the controls, and this finding indicates that the 11-MUA Au-NCs@SiO_2-FA were harmless fluorescent probes applicable for long-term imaging of living cells.

4. Conclusion

In summary, a novel, water-soluble, monodispersed, easily purified, fluorescent Au@SiO_2 nanocomposite was prepared via a simple water-in-oil microemulsion method. Furthermore, this investigation showed that the fluorescent nanocomposite bound to the FA can specifically target cancer cells' overexpressing folic acid receptors (FARs) and successfully label FARs in living cells within a short period of incubation. We further demonstrated that the fluorescent nanocomposites have significant cell viability for long-term cellular imaging. Additionally, because they are less cytotoxic and hold fluorescence properties, these new biomaterials may be further conjugated with other biomolecules, such as antibody, peptides, and aptamer, hence providing a unique platform for target imaging of other biological systems.

Acknowledgements

The National Natural Science Foundation of China (20890022) and the Shanghai Leading Academic Discipline Project (B109) supported this work.

References

[1] F. Tang, F. He, H. Cheng, L. Li, Langmuir 14 (2010) 11774.
[2] Y. Liu, K. Ai, X. Cheng, L. Huo, L. Lu, Adv. Funct. Mater. 6 (2010) 951.
[3] C. Chen, W. Chen, C. Liu, L. Chang, Y. Chen, Chem. Commun. 48 (2009) 7515.
[4] Y. Bao, H. Yeh, C. Zhong, S.A. Ivanov, J.K. Sharma, M.L. Neidig, D.M. Vu, A.P. Shreve, R.B. Dyer, J.H. Werner, J.S. Martinez, J. Phys. Chem. C 38 (2010) 15879.
[5] Y. Negishi, K. Nobusada, T. Tsukuda, J. Am. Chem. Soc. 14 (2005) 5261.
[6] S. Link, M.A. El-Sayed, T. Gregory Schaaff, R.L. Whetten, Chem. Phys. Lett. 3–4 (2002) 240.
[7] X. Liu, C. Li, J. Xu, J. Lv, M. Zhu, Y. Guo, S. Cui, H. Liu, S. Wang, Y. Li, J. Phys. Chem. C 29 (2008) 10778.
[8] C. Huang, C. Chen, Y. Shiang, Z. Lin, H. Chang, Anal. Chem. 3 (2009) 875.
[9] C. Huang, Z. Yang, K. Lee, H. Chang, Angew. Chem. Int. Ed. 36 (2007) 6824.
[10] M.A. Habeeb Muhammed, T. Pradeep, Small 2 (2011) 204.
[11] C.J. Lin, T. Yang, C. Lee, S.H. Huang, R.A. Sperling, M. Zanella, J.K. Li, J. Shen, H. Wang, H. Yeh, W.J. Parak, W.H. Chang, ACS Nano 2 (2009) 395.
[12] M. Darbandi, R. Thomann, T. Nann, Chem. Mater. 23 (2005) 5720.
[13] M. Cho, K. Lim, K. Woo, Chem. Commun. 30 (2010) 5584.
[14] S. Liu, Z. Zhang, Y. Wang, F. Wang, M. Han, Talanta 3 (2005) 456.
[15] Y. Chen, T. Ji, Z. Rosenzweig, Nano Lett. 5 (2003) 581.
[16] J. Lee, Y. Choi, K. Kim, S. Hong, H. Park, T. Lee, G.J. Cheon, R. Song, Bioconjugate Chem. 5 (2010) 940.
[17] N. Insin, J.B. Tracy, H. Lee, J.P. Zimmer, R.M. Westervelt, M.G. Bawendi, ACS Nano 2 (2008) 197.
[18] L. Zhou, C. Gao, X. Hu, W. Xu, ACS Appl. Mater. Interfaces 4 (2010) 1211.
[19] T.C. King-Heiden, P.N. Wiecinski, A.N. Mangham, K.M. Metz, D. Nesbit, J.A. Pedersen, R.J. Hamers, W. Heideman, R.E. Peterson, Environ. Sci. Technol. 5 (2009) 1605.
[20] J. Li, J.R. Anema, Y. Yu, Z. Yang, Y. Huang, X. Zhou, B. Ren, Z. Tian, Chem. Commun. 7 (2011) 2023.
[21] Y. Liu, K. Yang, T. Hsu, J. Phys. Chem. C 19 (2009) 8162.
[22] A. Cao, Z. Ye, Z. Cai, E. Dong, X. Yang, G. Liu, X. Deng, Y. Wang, S. Yang, H. Wang, M. Wu, Y. Liu, Angew. Chem. Int. Ed. 17 (2010) 3022.
[23] A.W. Snow, E.E. Foos, M.M. Coble, G.G. Jernigan, M.G. Ancona, Analyst 9 (2009) 1790.
[24] H. Tan, T. Zhan, W.Y. Fan, J. Phys. Chem. B 43 (2006) 21690.
[25] J. Liu, L. Zhang, S. Shi, S. Chen, N. Zhou, Z. Zhang, Z. Cheng, X. Zhu, Langmuir 18 (2010) 14806.
[26] H. Duan, S. Nie, J. Am. Chem. Soc. 9 (2007) 2412.
[27] P. Zhong, Y. Yu, J. Wu, Y. Lai, B. Chen, Z. Long, C. Liang, Talanta 4 (2006) 902.
[28] X. Zhao, Y. Cai, T. Wang, Y. Shi, G. Jiang, Anal. Chem. 23 (2008) 9091.
[29] P. Florian, K.K. Jena, S. Allauddin, R. Narayan, K.V.S.N. Raju, Ind. Eng. Chem. Res. 10 (2010) 4517.
[30] S. Lin, N. Chen, S. Sum, L. Lo, C. Yang, Chem. Commun. 39 (2008) 4762.
[31] H. Yang, Y. Zhuang, H. Hu, X. Du, C. Zhang, X. Shi, H. Wu, S. Yang, Adv. Funct. Mater. 11 (2010) 1733.
[32] M. Colilla, I. Izquierdo-Barba, S. Sánchez-Salcedo, J.L.G. Fierro, J.L. Hueso, M. Vallet-Regí, Chem. Mater. 23 (2010) 6459.
[33] M. Qhobosheane, S. Santra, P. Zhang, W. Tan, Analyst 8 (2001) 1274.
[34] S. Sadasivan, E. Dujardin, M. Li, C. Johnson, S. Mann, Small 1 (2005) 103.
[35] S. Sam, L. Touahir, J. Salvador Andresa, P. Allongue, J.N. Chazalviel, A.C. Gouget-Laemmel, C. Henry De Villeneuve, A. Moraillon, F. Ozanam, N. Gabouze, S. Djebbar, Langmuir 2 (2010) 809.
[36] L. Hosta-Rigau, I. Olmedo, J. Arbiol, L.J. Cruz, M.J. Kogan, F. Albericio, Bioconjugate Chem. 6 (2010) 1070.
[37] S. Nayak, H. Lee, J. Chmielewski, L.A. Lyon, J. Am. Chem. Soc. 33 (2004) 10258.